Figure 5
Click here to download Figure: Pondrelli_Fig5-print.pdf

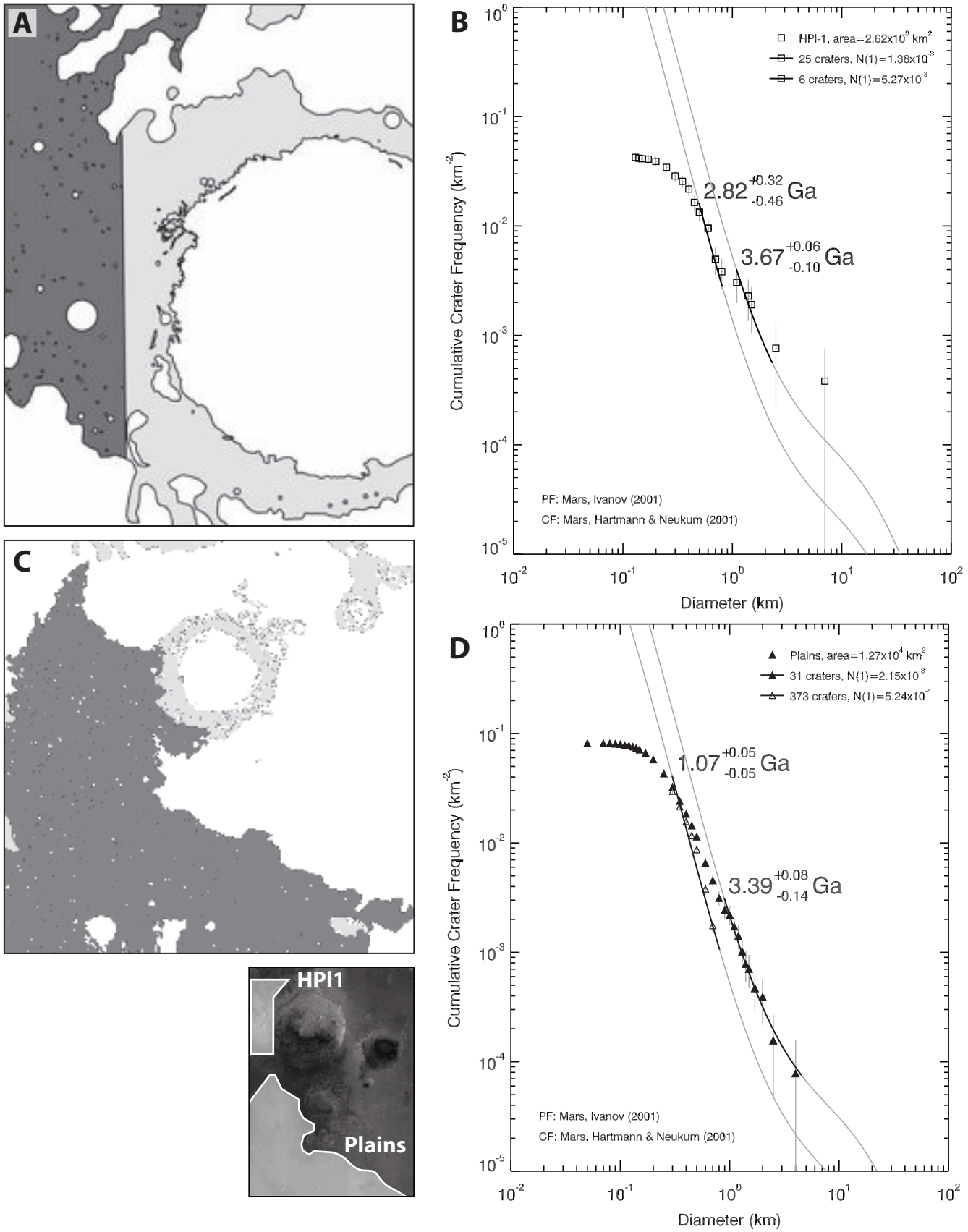

Figure 5. Crater size-frequency distribution results. (A) Excerpt of the geological map with outlined in dark grey the area where crater size frequency measurements have been performed in the HPl1 unit (see the down left HRSC mosaic for location). (B) Crater size frequency measurements of the area shown in (A). Isochrones plot based upon crater chronology model by Hartmann and Neukum [2001] and production function coefficients by Ivanov [2001]. See text for discussion. (C) Excerpt of the geological map with outlined in dark grey the area where crater size frequency measurements have been performed in the plains (see the down left HRSC mosaic for location). (D) Crater size frequency measurements of the area shown in (C). Isochrones plot based upon crater chronology model by Hartmann and Neukum [2001] and production function coefficients by Ivanov [2001]. See text for discussion.

Figure 6
Click here to download Figure: Pondrelli_Fig6-print.pdf

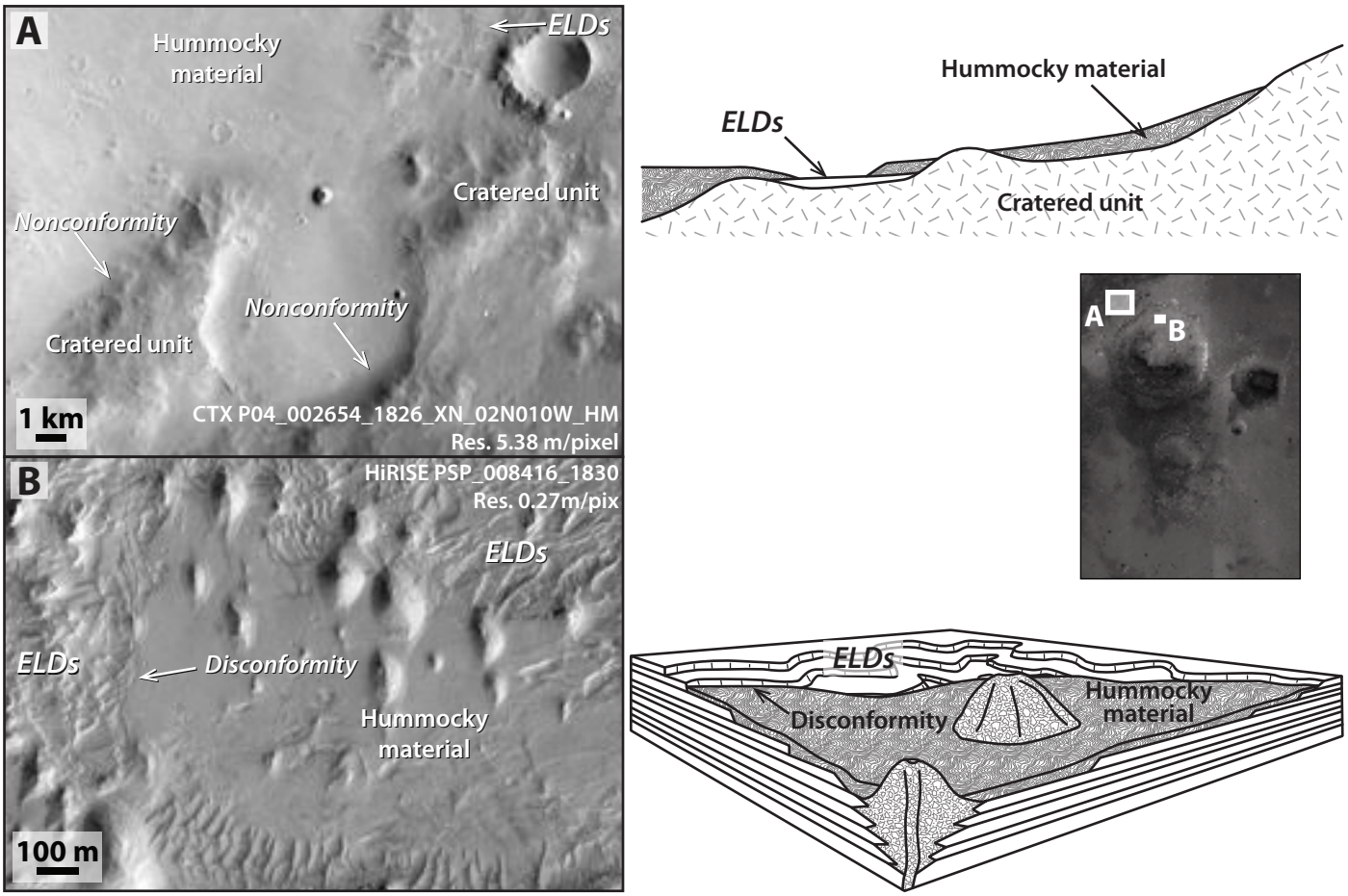

Figure 6. Stratigraphic relations. (A) CTX image showing the stratigraphic relations between the Cratered unit, the ELDs and the Hummocky material north of Firsoff crater (see the HRSC-based mosaic located at the center-right for location). The Hummocky material stays in nonconformity on top of the Cratered unit and in disconformity on top of the ELDs. Stratigraphic relations and geometries are sketched at the upper right of the image. (B) HiRISE image showing the stratigraphic relations between the ELDs and the Hummocky material inside Firsoff crater (see the HRSC-based mosaic located at the center-right for location). ELDs consist of layers and mounds and are covered in disconformity by the Hummocky material. Stratigraphic relations and geometries are sketched in the block diagram at the lower right of the image.

Figure 7
Click here to download Figure: Pondrelli_Fig7-print.pdf

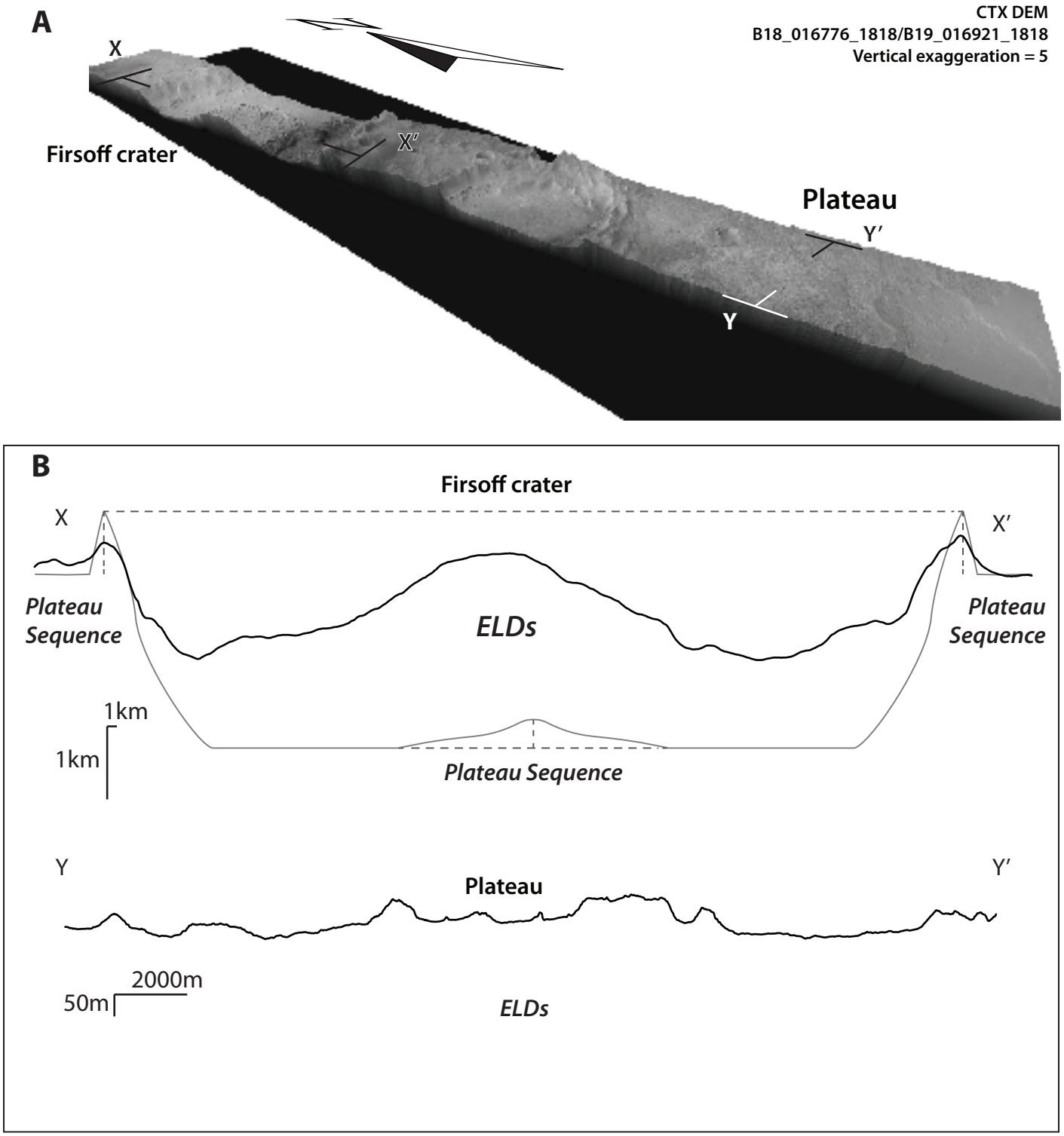

Figure 7. Geometries of the basins. (A) CTX-based 3D view across part of the study area with the trace of the profiles shown in B. (B) HRSC-derived profile XX′ though Firsoff crater and CTX-derived profile YY′ in the plateau. In the profile XX′, the inferred approximate morphology of the crater devoid of ELDs and other possible deposits (Garvin et al., 2003) is reconstructed in light grey. See text for description.

Figure 8
Click here to download Figure: Pondrelli_Fig8-print.pdf

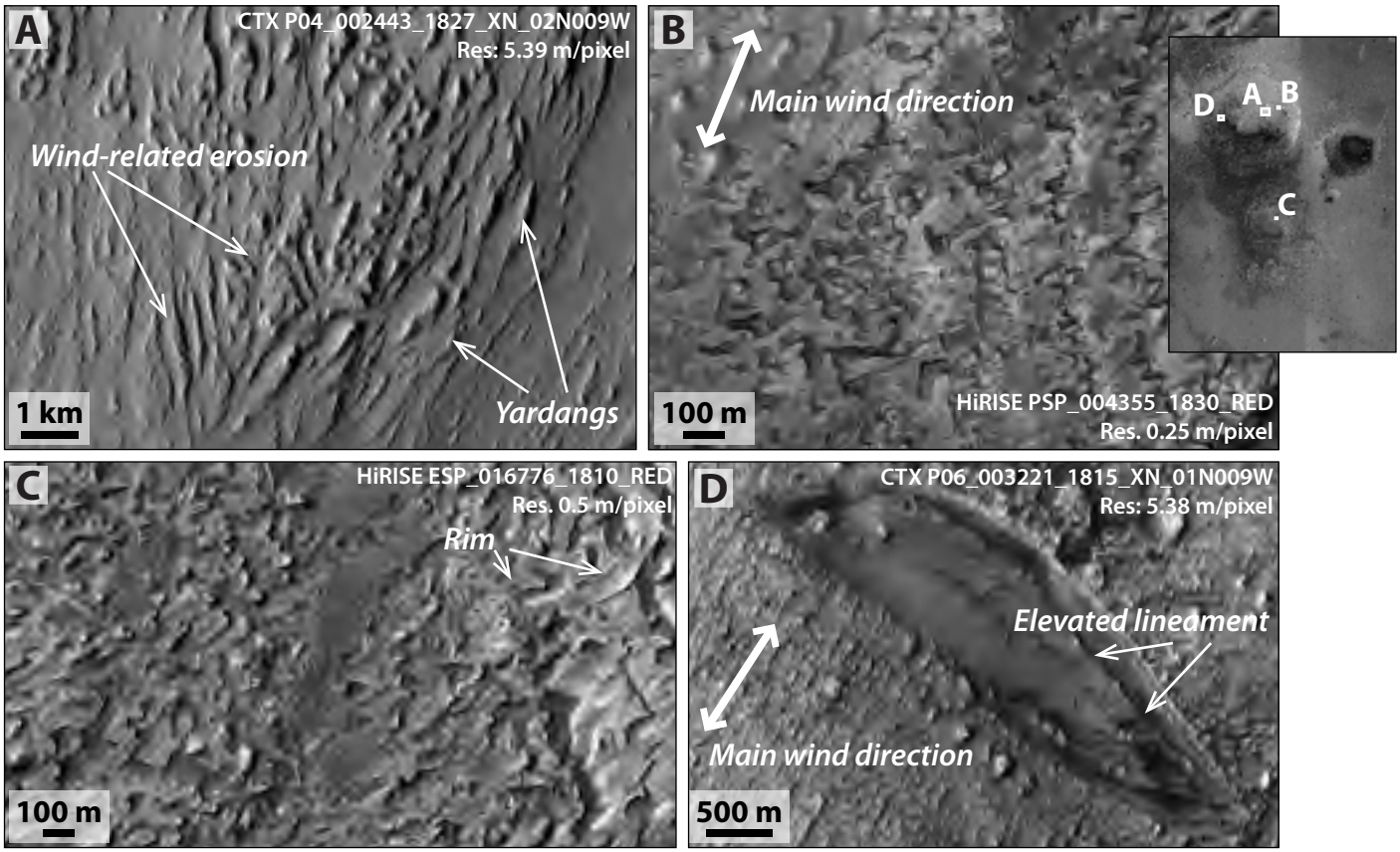

Figure 8. Erosional vs depositional morphologies. (A) Example of aeolian erosion with yardangs on ELDs. (B) ELDs irregularly shaped layers. ELDs show rounded shaped edges and lengthen in a direction and with geometries not consistent with a formation by aeolian erosion. Main wind direction as inferred by yardangs alignment is indicated top left in the figure. (C) ELDs irregularly shaped layers. Some of the layers are characterized by the presence of rims. (D) NW-SE trending depression. Its regularity and trend do not seem consistent with an erosional formation by wind action. Main wind direction as inferred by yardangs alignment is located to the bottom left of the figure. Inside the depression, elevated lineaments (possible fissure ridges?) emphasized by mounds, are present. The location of the images is indicated in the top right HRSC mosaic.

Figure 9
Click here to download Figure: Pondrelli_Fig9-print.pdf

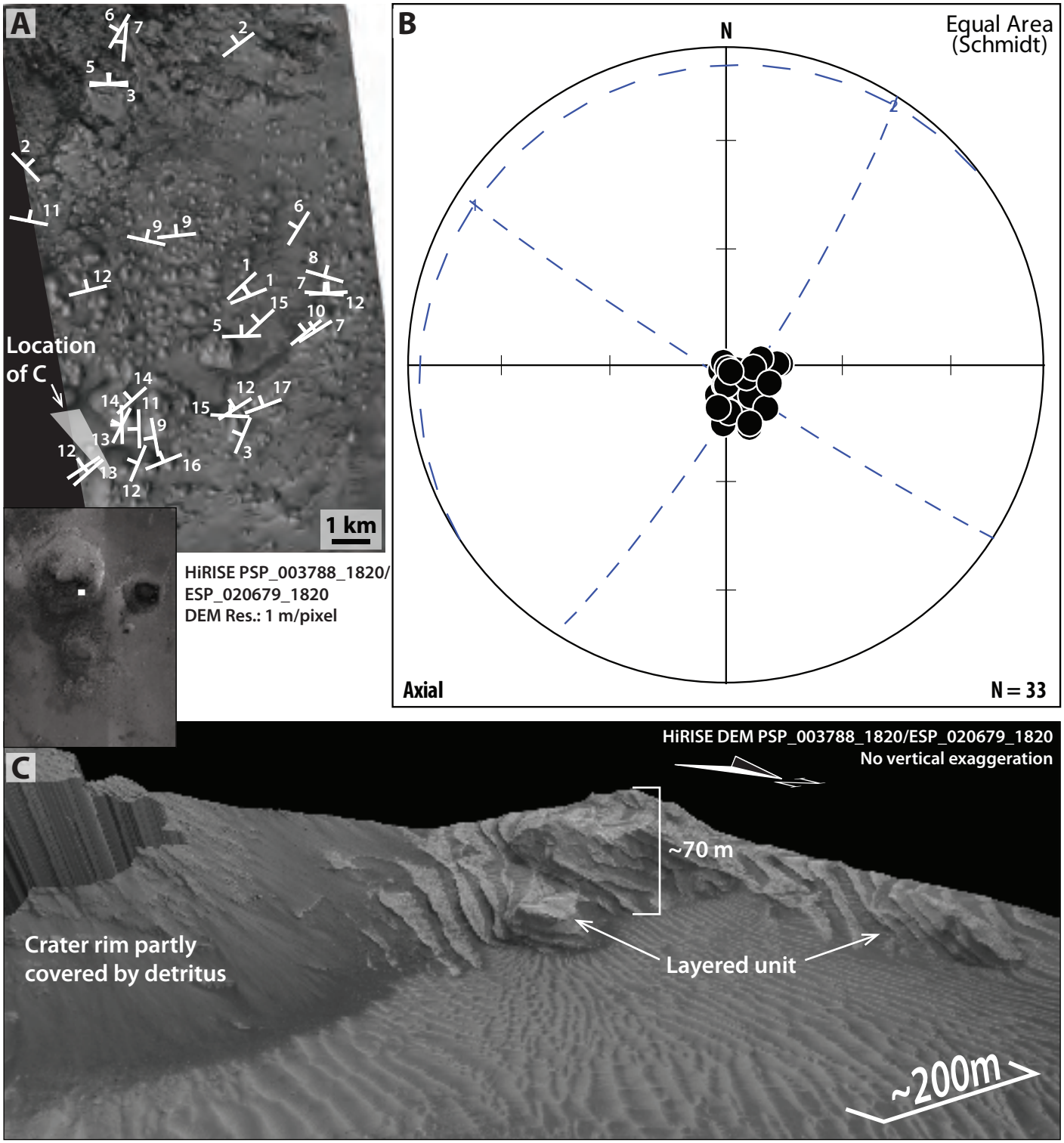

Figure 9. Layer attitude in the ELDs layered unit located in the south-eastern part of Firsoff crater. (A) HiRISE based map with the measured layer attitudes. The location of the image is indicated in the HRSC mosaic shown in the lower left inset. The white-transparent box in the lower left part of the figure represents the location of C. (B) Stereonet representing attitude values. The diagram shows a tight cluster but a definite preferred orientation. (C) Layered unit material draping Crater rim deposits. Note the absence of cross stratification at the scale of the available resolution. See A for location.

Figure 10
Click here to download Figure: Pondrelli_Fig10-print.pdf

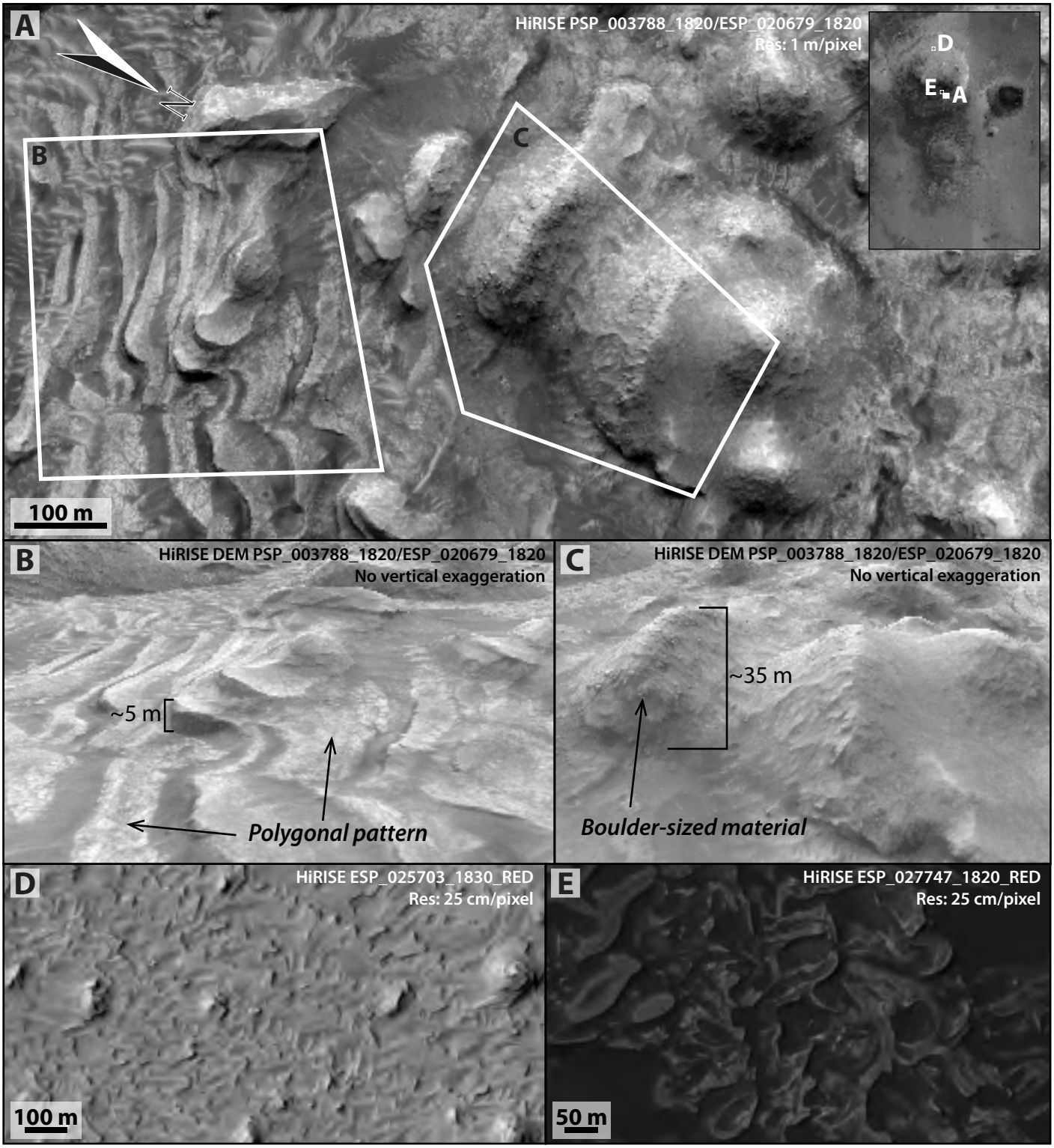

Figure 10. ELDs units. (A) HiRISE image showing the two units which make the ELDs: layered high albedo deposits disrupted in polygonal pattern and mounds made of either matrix- or clast-supported boulder-sized material. The two white polygons represent the approximate location of B and C. (B) Example of the layered unit. (C) Example of mounds. (D) Layered unit showing layer morphologies. (E) Depressions, raised rims and layer morphologies. The location of the image is indicated in the top right HRSC mosaic.

Figure 11
Click here to download Figure: Pondrelli_Fig11-print.pdf

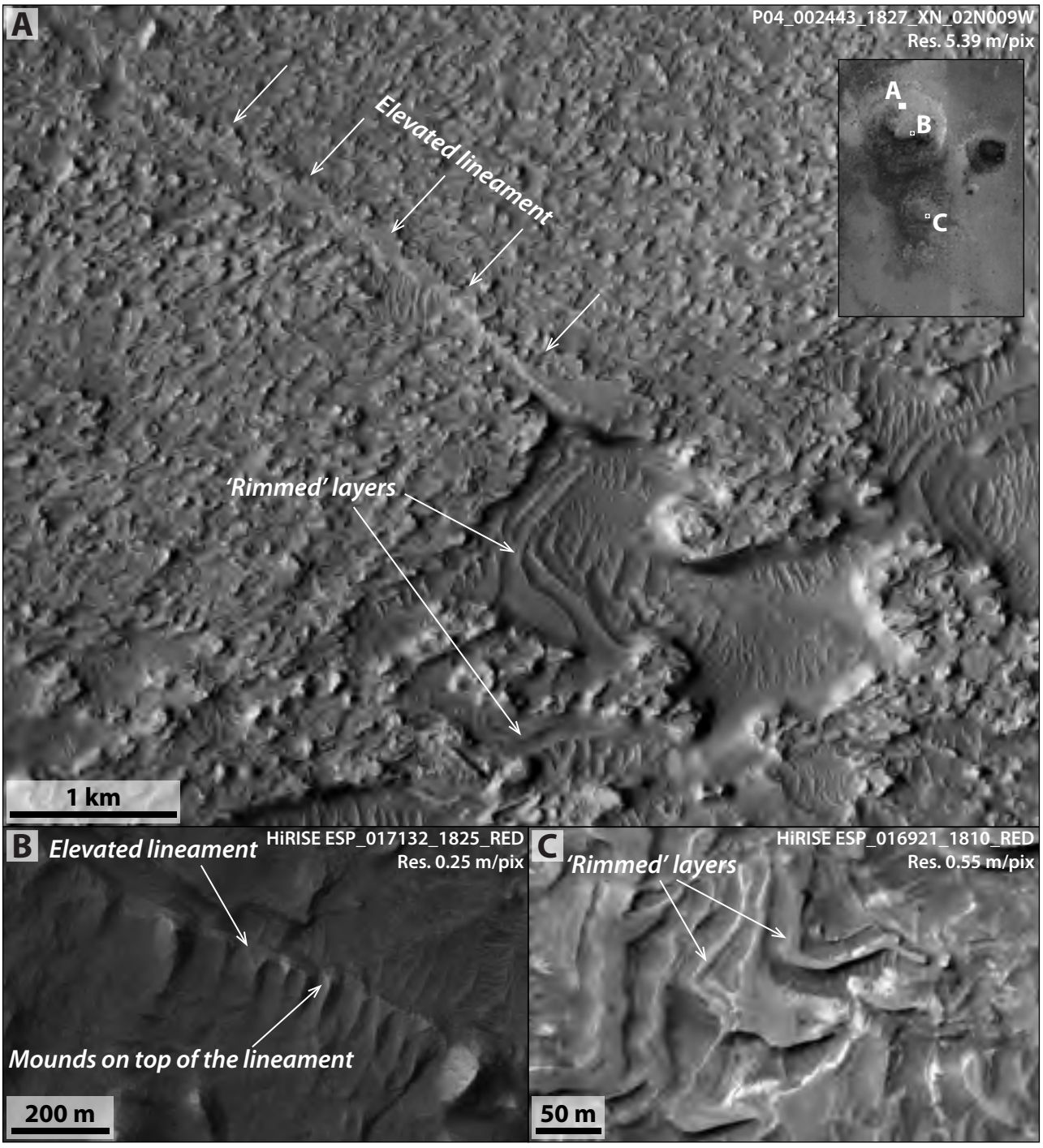

Figure 11. ELDs morphologies. (A) CTX image showing an example of elevated lineament (possible fissure ridge). Material appears to source from the subsurface in correspondence of a tectonically-controlled fracture. ELDs layers appear to be bounded by a rim. (B) Example of an elevated lineament (possible fissure ridge) with mounds developing on the top. (C) Example of ELDs layers which seem to be bounded by a rim. The location of the images in (A), (B) and (C) is indicated in the top right HRSC mosaic.

Figure 12
Click here to download Figure: Pondrelli_Fig12-print.pdf

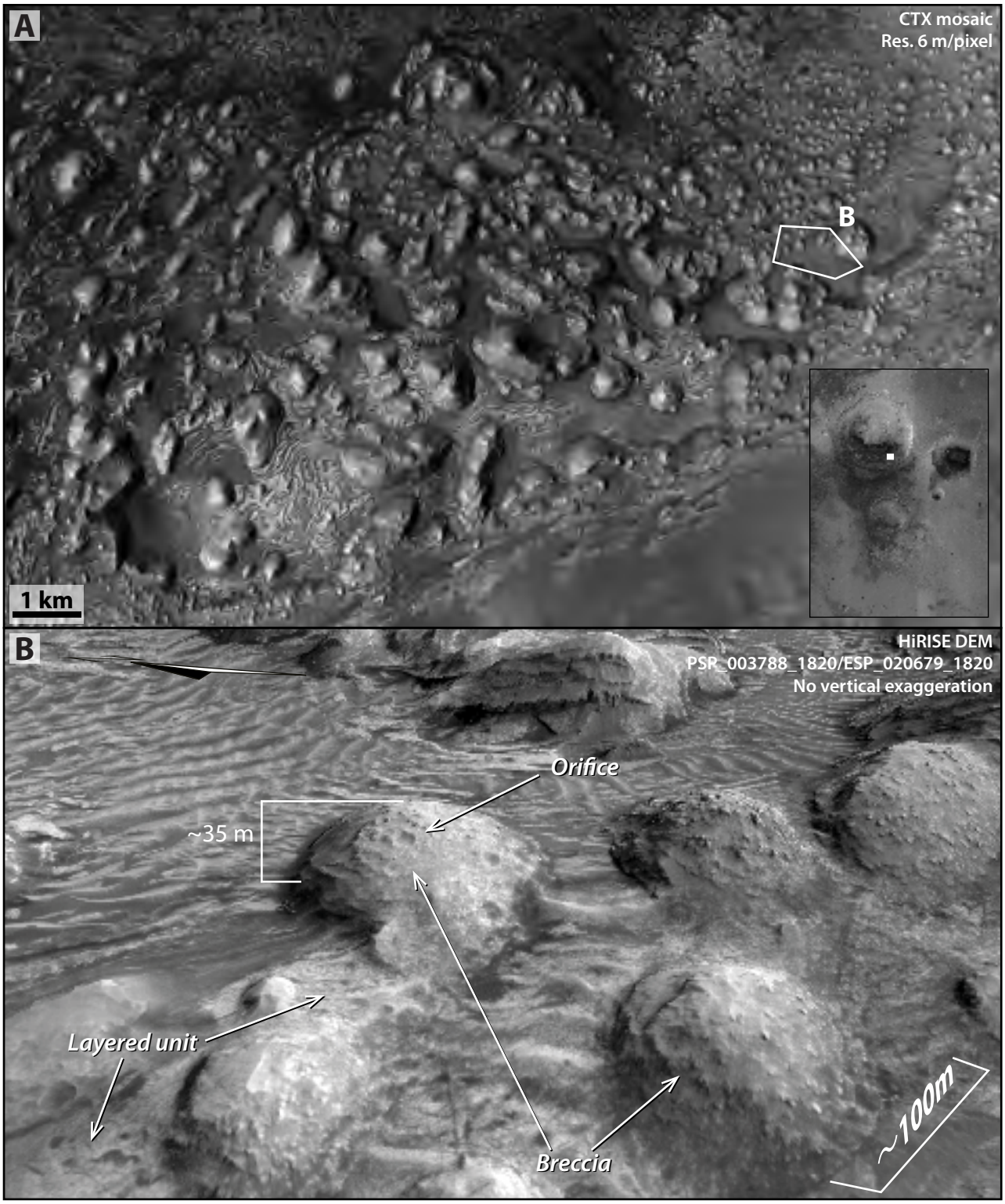

Figure 12. Mounds. (A) Field of simple and complex mounds in the southern part of Firsoff crater (see inset for location). Location of B is shown by the white-bounded polygon. (B) HiRISE-derived 3D view of simple mounds.

Figure 13
Click here to download Figure: Pondrelli_Fig13-print.pdf

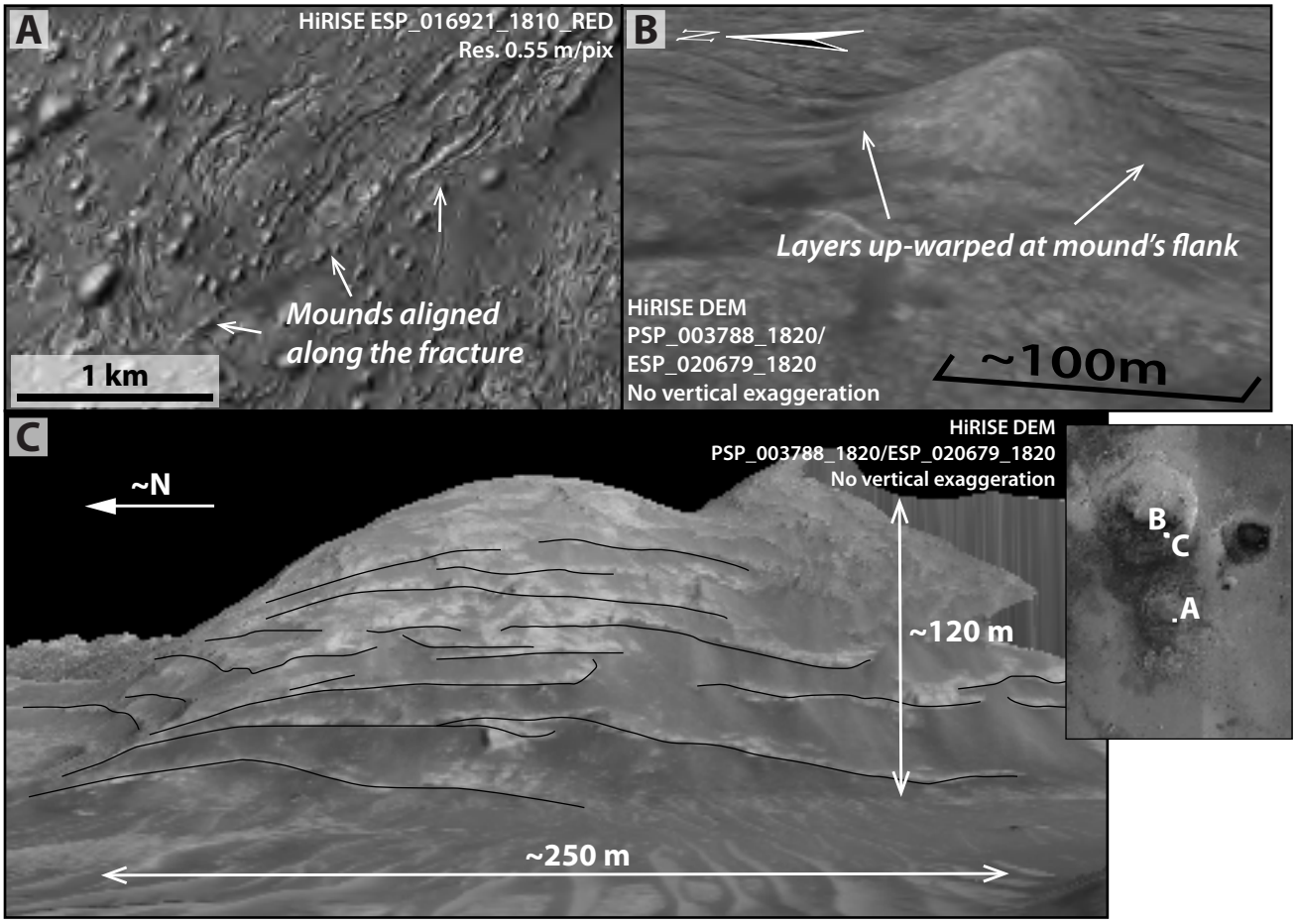

Figure 13. (A) Example of mounds aligned along fractures and not (redrawn after Franchi et al., 2014). (B) Layers up-warped at the flanks of the mounds. (C) Depositional geometry of a mound and relation with the layered unit. Layers continue from the mounds to the layered unit, suggesting facies heteropy between the units. The location of the images is indicated in the HRSC mosaic shown in the lower right corner.

Figure 14
Click here to download Figure: Pondrelli_Fig14-print.pdf

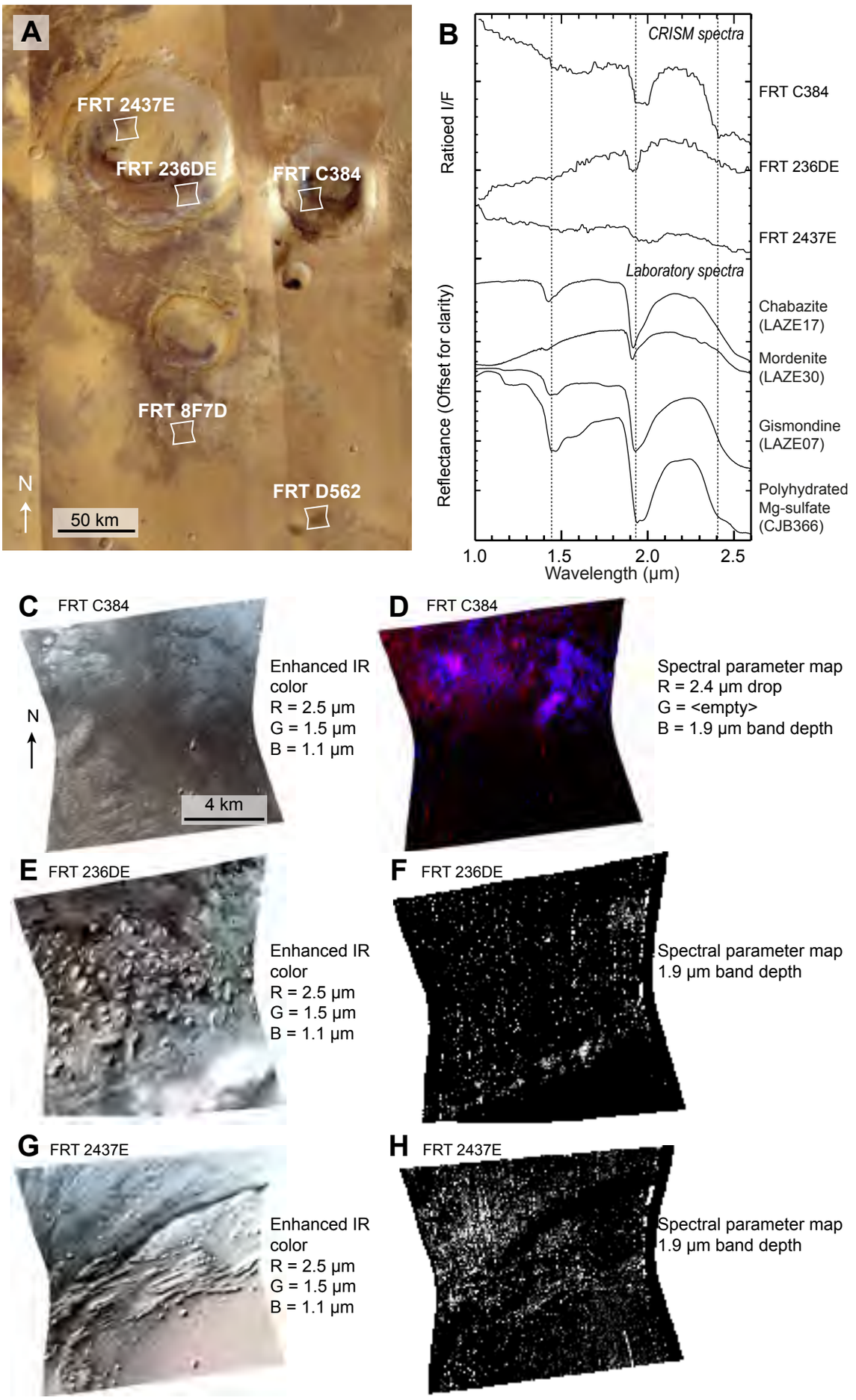

Figure 14. Sulfate-rich deposits in the study area. (A) Subset of HRSC nadir mosaic overlain by CRISM footprints of observations showing sulfates in craters. Observations on plateaus possibly display hydrated minerals. (B) CRISM ratioed spectra compared to laboratory spectra of zeolites and polyhydrated sulfates (RELAB library spectrum). The ratioed spectrum of the CRISM observation FRT C384 corresponds to an average of 30 pixels divided by an average of 35 pixels of a neutral region. It corresponds to an average of 32 pixels divided by 25 pixels for the observation FRT 236DE, and of 4677 by 356 for the observation FRT 2437E. (C) False color image of the CRISM observation FRT C384. (D) Spectral parameter map of the same observation (red, SINDEX; blue, BD1900R). Displayed values: red, 0.037-0.054; blue, 0.014–0.024. Pink tones indicate occurrence of polyhydrated sulfates, and blue tones of hydrated phases. (E) False color image of the CRISM observation FRT 236DE. (F) Spectral parameter map of the same observation (BD1900R). Displayed values: 0.002–0.010. White tones indicate occurrence of hydrated phases. (G) False color image of the CRISM observation FRT 2437E. (H) Spectral parameter map of the same observation (BD1900R). Displayed values: 0.003–0.010. White tones indicate occurrence of hydrated phases.

Figure 15
Click here to download Figure: Pondrelli_Fig15-print.pdf

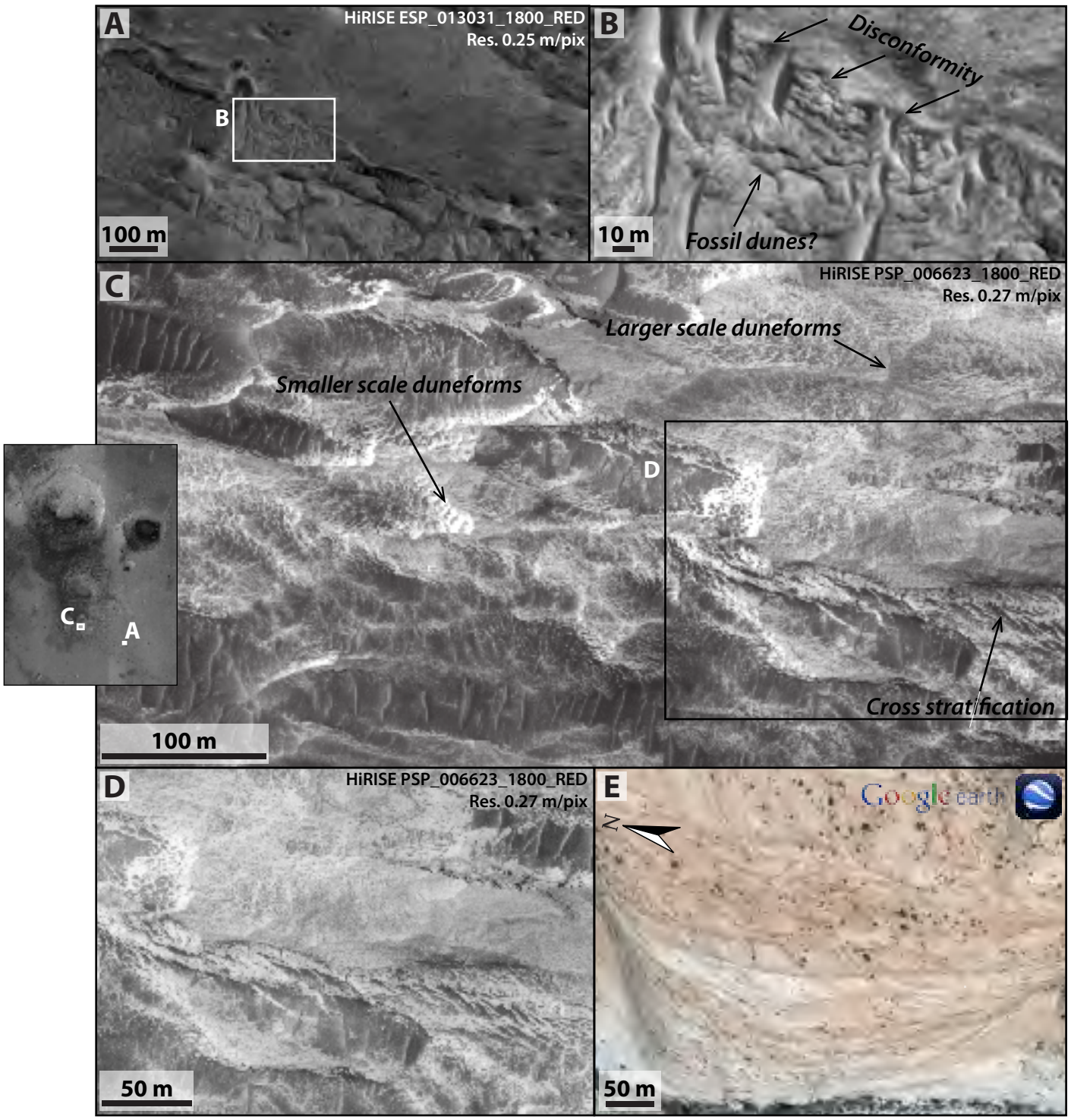

Figure 15. Example of ELDs on the plateau. The location of the images is indicated in the left HRSC mosaic. (A) Flat-lying bedded to faintly bedded deposits. The boxed area represents the location of B. (B) ELDs on the plateau are characterized by high albedo and are disrupted in polygonal pattern as in the craters. Possible dune deposits are covered in disconformity by flat-lying bedded deposits. (C) Bedded deposits associated with dune-fields. The boxed area represents the location of D. (D) Meter-scale cross-stratification (see text for discussion). (E) Example of meter-scale cross-stratification from the Early Jurassic Navajo Sandstone (southern Utah, USA). Google Earth image (centered lat. 37°11'22.81"N, long. 112°57'16.73"W), used with permission.

Figure 16
Click here to download Figure: Pondrelli_Fig16-print.pdf

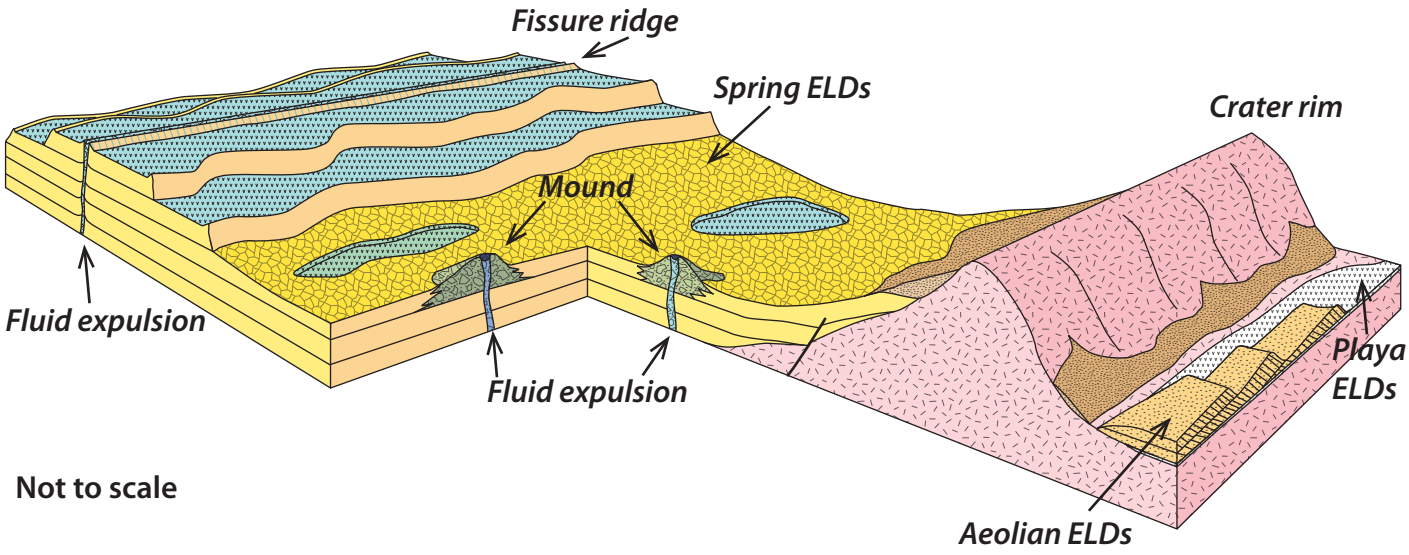

Figure 16. Processes inferred to have caused ELDs formation. ELDs inside craters (in yellow) are interpreted as formed by fluid expulsion and spring deposits precipitation. In blue areas possibly submerged by waters are indicated. ELDs outside craters were probably subjected in part to aeolian reworking (light brown) and in part to playa deposition (white).

Figure 17
Click here to download Figure: Pondrelli_Fig17-print.pdf

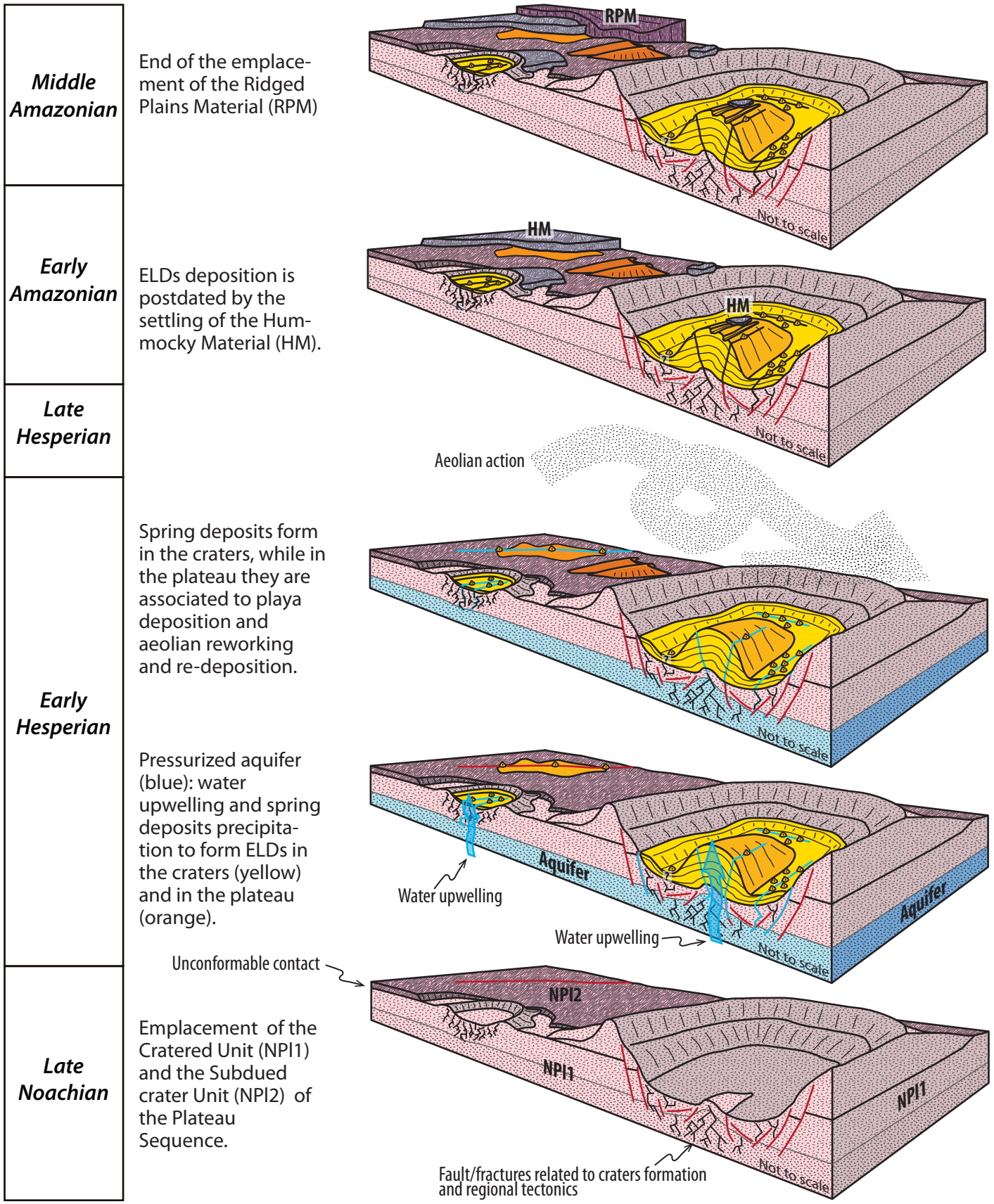

Figure 17. Interpretative scenario of the evolution of the study area through time. From bottom to top the evolution from the Late Noachian to the Middle Amazonian is sketched. See text for explanation.

Table 1

Setting	Crater		Plateau		
Architecture of the ELDs	**Bulges**		**Sheet drapes**		
Stratal pattern	Draping, onlapping		Draping, onlapping		
Units	Layered unit	Mounds	Mounds	Flat-lying bedded to faintly bedded deposits	Bedded deposits associated with dune-fields
Textures and Sedimentary structures	Layering; Polygonal pattern	Layering; Breccia	Uncertain	Layering; Polygonal pattern	Layering; Cross-bedding
Morphologies	Fissure ridges; etched terrains*; dish-shaped depressions, raised rims, bowl-shaped appearance; serrated layer morphology	Pitted cones; Fissure ridges	Conical shape; Pitted?	Flat bodies; etched terrains*; Fissure ridges	Dune-fields

* Hynek et al., 2002